Available online at www.sciencedirect.com
ScienceDirect
Ceramics International 35 (2009) 327–332
CERAMICS INTERNATIONAL
www.elsevier.com/locate/ceramint

Crystallization kinetics of lanthanum monoaluminate ($LaAlO_3$) nanopowders prepared by co-precipitation process

Chia-Liang Kuo [a], Yen-Hwei Chang [a], Moo-Chin Wang [b,*]

[a] Department of Materials Science and Engineering, National Cheng Kung University, 1 Ta-Hsueh Road, Tainan 70101, Taiwan
[b] Faculty of Fragrance and Cosmetics, Kaohsiung Medical University, 100 Shih-Chuan 1st Road, Kaohsiung 807, Taiwan

Received 16 July 2007; received in revised form 15 September 2007; accepted 30 October 2007
Available online 18 April 2008

Abstract

Lanthanum monoaluminate ($LaAlO_3$) nanopowders were synthesized using $La(NO_3)_3{\cdot}6H_2O$ and $Al(NO_3)_3{\cdot}6H_2O$ as starting materials by a co-precipitation method. The crystallization kinetics of the $LaAlO_3$ nanopowders has been investigated by using differential thermal analysis (DTA), X-ray diffraction (XRD), scanning electron microscopy (SEM), transmission electron microscopy (TEM) and selected area electron diffraction (SAED). The XRD results and SAED patterns show that the rhombohedral $LaAlO_3$ nanopowders have been obtained when the precipitates as calcined at 1092 K for 10 min. The activation energy for the crystallization of the rhombohedral $LaAlO_3$ nanopowders is determined as 286.75 kJ/mol by a non-isothermal method. The TEM examination shows that the rhombohedral $LaAlO_3$ has a spherical morphology with the size ranging from 30 to 50 nm.

Keywords: Crystallization kinetics; Lanthanum monoaluminum; Co-precipitation method; Thermal analysis

1. Introduction

Polycrystalline $LaAlO_3$ has been commonly prepared by a solid-state reaction method: i.e. direct mixing and firing of pure oxides of La_2O_3 and Al_2O_3 at temperature greater than 1823 K [1–4]. The full development of the $LaAlO_3$ phase has been exercised by only heating to 1873 K and then reheating to 2023 K for 3 h to form a polycrystalline disk. The preparation of a buffer disk of 123 nm thick $LaAlO_3$ by radio-frequency magnetron sputtering has also been reported by Sung et al. [2].

Although the solid-state reaction is very simple, this process is not entirely satisfactory because of several serious drawbacks such as introduction of impurities during milling, high reaction temperature, limit of complete oxide reaction and chemical homogeneity, large particle size and low sintering ability [5,6]. Pure $LaAlO_3$ powders have been synthesized at 1133 K using polyacrylamide by Douy and Odier [7].

Moreover, Taspinar and Tas [4] have also reported synthesized pure $LaAlO_3$ powders by calcining at 1023 K for 16 h, using a self-propagating combustion method from aqueous solutions containing CH_4N_2O and respective nitrates of lanthanum and aluminum. Furthermore, they have also synthesized pure $LaAlO_3$ powders at 1123 K by homogeneous precipitation from an aqueous solution containing CH_4N_2O in nitrate salts [4]. Kakihana and Okubo [8] have reported that in the polymerization route of citric acid and ethylene glycol, pure perovskite $LaAlO_3$ has been obtained when the precursor is heat-treated in a furnace at 973 K for 8 h or at 1023 K for 2 h. However, all these processes are either complex or expensive, and limit their large-scale production.

Therefore, extensive investigations have been performed for preparing finer and more homogeneous powders at lower temperatures using various chemical processes. On the other hand, Kuo et al. [9], have pointed out that nanoscaled lanthanum monoaluminate powders can be successfully synthesized by a wet-chemical co-precipitation method. $LaAlO_3$ precursor can transfer to rhombohedral structure of $LaAlO_3$ when calcined at 937 K for 6 h. Lanthanum aluminate powders can be synthesized by various methods [5,10,11], but the crystallization kinetic of $LaAlO_3$ has not been discussed in detail.

The thermal behavior of various materials has been investigated by a differential thermal analysis technique. For

* Corresponding author.
E-mail address: mcwang@kmu.edu.tw (M.-C. Wang).

0272-8842/$34.00
doi:10.1016/j.ceramint.2007.10.012

the crystallization and phase transition study of materials, DTA is useful in determining the transformation temperature. Many previous studies have provided a detailed analysis for the crystallization kinetics study by a non-isothermal DTA method, in which crystallization and growth mechanism can be elucidated [12].

In the present study, the crystallization kinetics of the $LaAlO_3$ nanopowders prepared by a co-precipitation process have been investigated by differential thermal analysis, X-ray diffraction (XRD), scanning electron microscopy (SEM), transmission electron microscopy (TEM), and selected area electron diffraction (SAED). The purpose of this work is to investigate the phase transformation and crystallization kinetics of $LaAlO_3$ nanopowders.

2. Experimental procedure

2.1. Sample preparation

The starting materials were reagent-grade lanthanum nitrate [$La(NO_3)_3{\cdot}6H_2O$, purity ≧98%, supplied by Alfa Aersar, USA], aluminum nitrate [$Al(NO_3)_3{\cdot}9H_2O$, purity 99.9%, supplied by Riedel-de Haën, Germany], and 25 vol% ammonia solution (supplied by Riedel-de Haën). The 0.5 M aqueous solution was prepared from reagent-grade $La(NO_3)_3{\cdot}6H_2O$ and $Al(NO_3)_3{\cdot}9H_2O$ by dropping then slowly at a rate of 0.05 cm^3/min into the dilute ammonia solution (pH 12) with vigorous agitation. At the end of titration, a syringe was used to minimize the size of falling drops and reduce the local reaction effect. Through the whole process, the pH value was kept at 9 by adjusting the amount of NH_4OH to form white precipitates. After the reaction, the white precipitates were aged in the original liquid for 24 h and the resultant gelationous precipitates were then washed thoroughly four times with a distilled water–ammonia solution containing a small amount of ammonia as a washing agent to remove nitrates. Subsequently, the precipitates were repeatedly washed with water and ethanol three times and then frozen at 218 K in vacuum.

The $LaAlO_3$ precursor was calcined in an Al_2O_3 boat at 883–1083 K for 10 min and finally cooled to room temperature at a rate of 5 K/min.

2.2. Sample characterization

DTA (Setsys evolution, Setrum, France) was conducted in the temperature range of 323–1273 K in static air. The 50 mg $LaAlO_3$ precursor powders were heated at various heating rates. A platinum boat was used as a reference material. The calcination temperature was determined from the DTA curve.

The crystalline phase was identified by h a Rigaku X-ray diffractometer (Model Rad II A, Rigaku, Tokyo, Japan) with Cu Kα radiation and a Ni filter, operating at 30 kV, 20 mA and a scanning rate of 0.25° min^{-1}.

The morphology of the calcined $LaAlO_3$ powders was examined by a scanning electron microscope (SEM, Model S-4200, Hitachi Ltd., Tokyo, Japan) and a transmission electron microscope (TEM, H700H, Hitachi, Japan) operating at 200 kV. Selected area electron diffraction examination was also made on the TEM sample.

3. Result and discussion

3.1. Thermal behavior and phase formation of the $LaAlO_3$ gel powders

Fig. 1 reveals three main endothermic events at 358, 486 and 723 K, respectively. At the temperature below 358 K, 9.23% weight loss is assigned to the loss of moisture from the washed precursor powders. Apparently, the endothermic peak at 486 K with 18.38% weight loss is due to the dehydration of the precursor powders. The third endothermic peak at 723 K with 11.80% (total 30.18%) weight loss is attributed to the decomposition of NH_4^+ into N_2 and H_2. The exothermic peak around 993 K is due to the pyrolysis occurring in further heating of the precursor sample [10]. The sharp exothermic peak at 1083 K is due to the formation of the $LaAlO_3$. The crystallization kinetics study of the $LaAlO_3$ powders was evaluated using DTA analysis with various heating rates. Fig. 2 shows the DTA curves for the crystallization of the $LaAlO_3$ powders at various heating rates, ranging from 10 to 40 K/min. It is found that the exothermic peak shifts to high temperature with increasing heating rate. This phenomenon suggests that irregular lanthanum and aluminum ions are rearranged into the periodic lattice of the growing crystal. When the heating rate increases the rearrangement is delayed to the high temperature side.

Fig. 3 illustrates the XRD patterns of the $LaAlO_3$ powders calcined at different temperatures for 10 min. The XRD pattern of the $LaAlO_3$ powders calcined at 883 K for 10 min is shown in Fig. 3(a), which reveals that the calcined powders are still amorphous. The XRD pattern of the $LaAlO_3$ precursor calcined at 983 K for 10 min is illustrated in Fig. 3(b), indicating that the crystalline phase is the rhombohedral $LaAlO_3$ with poor crystallinity. The XRD pattern of the $LaAlO_3$ powders calcined at 1083 K for 10 min is shown in Fig. 3(c), in which the

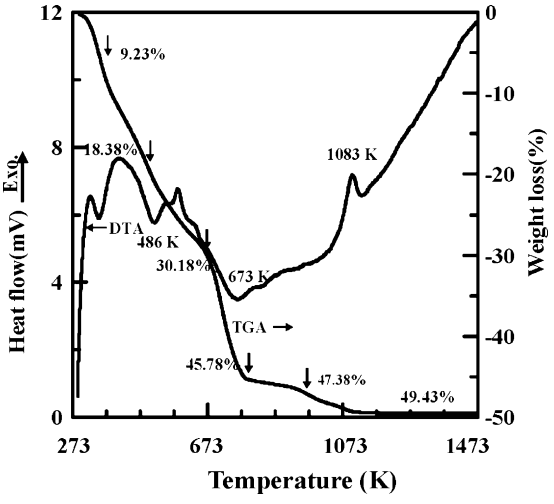

Fig. 1. DTA/TG curves of the $LaAlO_3$ precursor powders precipitated at pH 9 with a heating rate of 10 K/min.

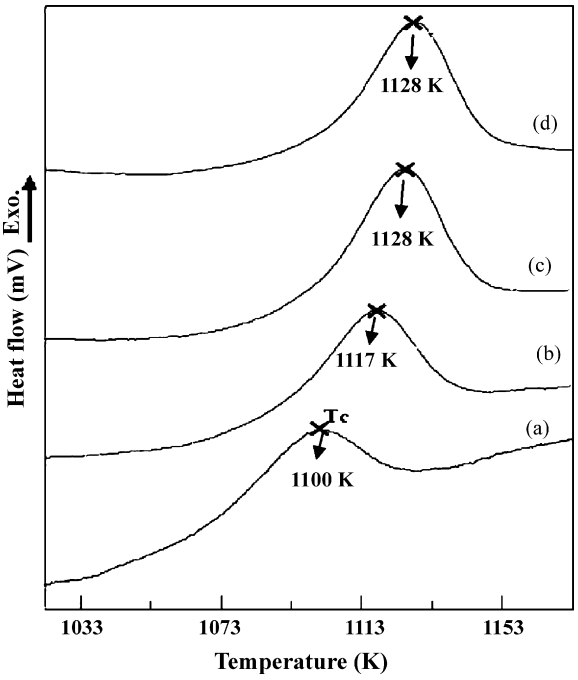

Fig. 2. Exothermic peak of DTA curves for $LaAlO_3$ powders in various heating rates: (a) 10 K/min, (b) 20 K/min, (c) 30 K/min and (d) 40 K/min.

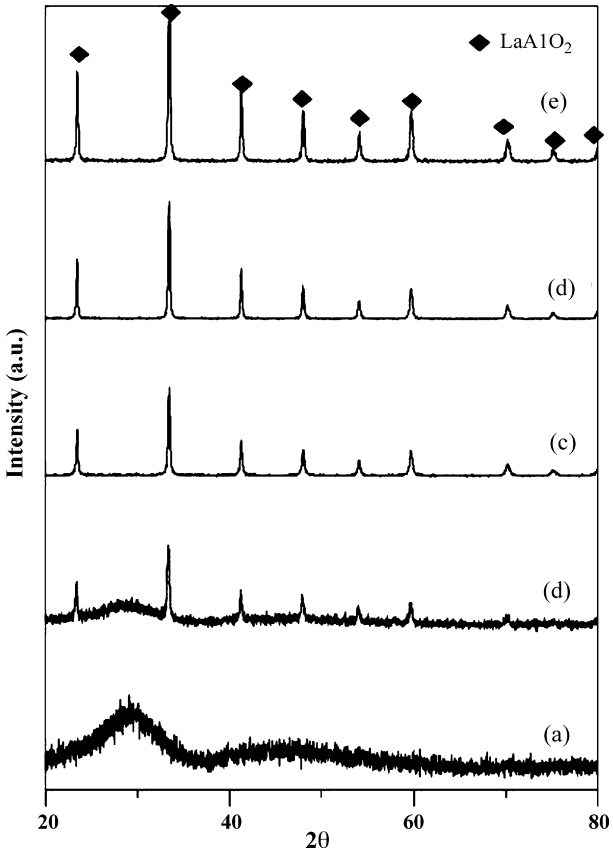

Fig. 3. XRD patterns of $LaAlO_3$ powders calcined at different temperatures for 10 min: (a) 883 K, (b) 983 K, (c) 1083 K, (d) 1183 K, and (e) 1283 K.

crystallinity of the rhombohedral of $LaAlO_3$ is remarkably improved. Moreover, the result of Fig. 3 also reconfirms that the exothermic peak of Fig. 1, spanning from 1043 to 1133 K, is due to the formation of the rhombohedral of $LaAlO_3$ nanopowders.

3.2. Crystallization kinetics and growth mechanism of the $LaAlO_3$ formation

DTA is widely used to study crystallization kinetics as a non-isothermal method [9]. The crystallization temperature, T_c, depends on heating rate, β, and their value is expressed by Arrhenius equation [5].

Johnson-Mehl-Avrami (JMA) equation could be applied for deriving the non-isothermal activation energy of $LaAlO_3$ nanopowders [13].

$$\ln \beta = -\frac{E_c}{R} \times \frac{1}{T_c} + \ln \mathrm{CM} \quad (1)$$

where E_c is the apparent activation energy for crystallization, R denotes the universal gas constant and ln CM is a constant.

From the result of the DTA curves at various heating rates, a linear relation holds between ln β and $1/T_c$ as demonstrated in Fig. 4. Thus, the apparent activation energy is obtained from the slope of the fitted straight line, as 286.75 kJ/mol.

When a sample is crystallized in a DTA run, the exothermic peak is related to the growth morphology parameter (n). The higher n value the narrower the peak. The DTA curve shows a narrower peak at a higher heating rate of 10 K/min as shown in Fig. 3. An enlarged view of the exothermic peak (T_c) is shown in Fig. 5. Since the heat evolved in a small time interval is directly proportional to the number of the related moles and the A_i deflection from the base line at any given instant is proportional to the instantaneous crystallization rate [14].

When the sample is heated at a constant rate, $dT/dt = \beta$, the total number of the cubic nuclei formed per unit volume, N, and

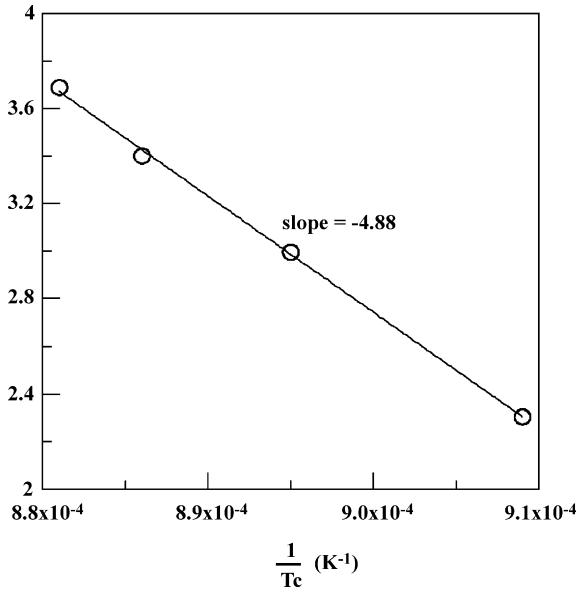

Fig. 4. Plot of ln β versus $1/T_c$.

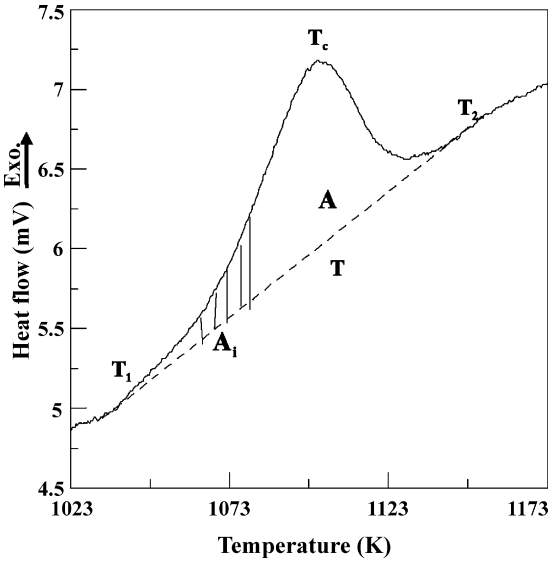

Fig. 5. An enlarged view of the DTA curve of $LaAlO_3$ powders obtained at a heating rate of 10 K/min.

the radius of the crystal particle, r, in the course of heating from room temperature (T_r) to T are expressed, respectively [17,16].

$$N = \frac{1}{\beta}\int_{T_r}^{T} I(T)\,\mathrm{d}T = \frac{N_0}{\beta} \tag{2}$$

$$r = \frac{1}{\beta}\int_{T_r}^{T} U(T)\,\mathrm{d}T \tag{3}$$

where N_0 is the initial number of nuclei. $I(T)$ and $U(T)$ denote the rates of nucleation and crystal growth, respectively. $U(T)$ can be expressed as [15,16]:

$$U(T) = \nu_0 \lambda \exp\left(-\frac{E_c}{RT}\right) = \mu_0 \exp\left(-\frac{E_c}{RT}\right) \tag{4}$$

where E_c means the activation energy for crystal growth, and ν_0 and λ denote the number of related atoms or molecules, trying to climb over an energy barrier in a second and the thickness of one atom layer, respectively.

The radius of the crystal partite, r, can be rewritten as [15,17]:

$$r = \frac{1}{\beta}\int_{T_r}^{T} \mu_0 \exp\left(-\frac{E_c}{RT}\right)\mathrm{d}T \approx \frac{r_0}{\beta}\exp\left(-\frac{E_c}{RT}\right) \tag{5}$$

where r_0 denotes the initial radius of the crystal particle.

There are two types of crystallization which take place in ceramics, based on bulk and surface nucleation. In the case of bulk nucleation, the volume fraction of the crystallite, α, is expressed as [17]:

$$\frac{\mathrm{d}\alpha}{\mathrm{d}t} = \frac{4N_0 r_0^{n-1}\mu_0}{\beta^n}(1-\alpha)\exp\left(-\frac{nE_c}{RT}\right) \tag{6}$$

where $\alpha = A_i/A$, A is the area under DTA curve between the phase formation-started temperature (T_1) and the phase formation-completed temperature (T_2), A_i is the area between T_1 and T_i and n is the growth morphology parameter as shown in Fig. 5.

In the case of surface nucleation, nuclei are formed only on the surface and the crystal grows from the surface to the inside one-dimensionally. The volume fraction of the crystallite is expressed as [17]:

$$1-(1-\alpha)^{1/3} = \frac{r}{R_0} = \frac{1}{\beta}\frac{r_0}{R_0}\exp\left(-\frac{E_c}{RT}\right) \tag{7}$$

where R_0 denotes the initial crystallite radius.

By using Eqs. (6) and (7), the following simplified Johnson-Mehl-Avrami expression is derived:

$$\log[-\ln(1-\alpha)] = -m\log\beta - \frac{1}{2.303}\frac{nE_c}{RT} + \text{constant} \tag{8}$$

where n means the growth morphology parameter, and m denotes the crystallization mechanism index. For the bulk nucleation and constant number of nuclei such as the three-dimensional growth, $m = 3$ and $n = 3$. For the two-dimensional growth, $m = 2$ and $n = 2$. For $m = n = 1$, it describes one-dimensional growth or surface nucleation from a constant number of nuclei.

The plot of $\log[-\ln(1-\alpha)$ against $1/T$ for the samples at various heating rates are shown in Fig. 6. The value of n is obtained from the slope of the fitted straight line where E_c is determined by Eq. (4). The calculated value of n decreases with increasing heating rate as listed in Table 1. It is found that n is 3.42 at a heating rate of 10 K/min, and decreases gradually to 3 as the heating rate increases to 40 K/min, in which the initial crystallization mechanism is characterized by instantaneous nucleation. Within an experimental error, the average value is approximated to 3. The non-isothermal result with a reaction order n of 3 is attained.

Fig. 7 reveals the plots of $\log[-\ln(1-\alpha)$ versus $\log\beta$ for the crystallization in $LaAlO_3$ at various temperatures. According to Eq. (8), m value could be determined for the formation of $LaAlO_3$ at various temperatures as shown in Table 1 and those

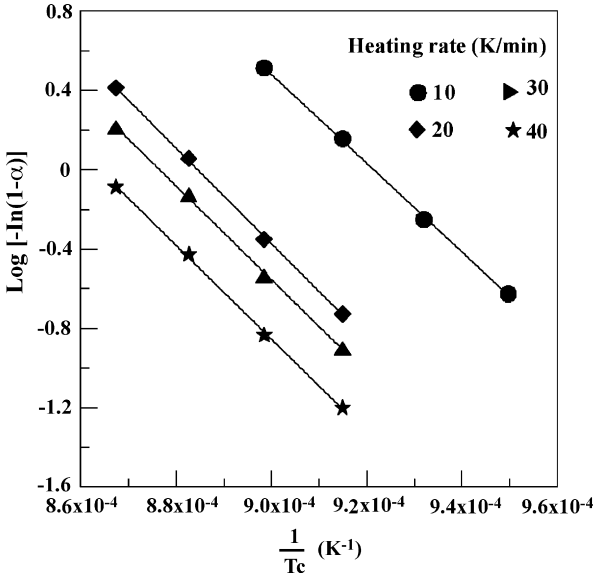

Fig. 6. Plots of $\log[-\ln(1-\alpha)$ versus $1/T$ at various heating rate.

Table 1
Growth morphology parameters n and crystallization mechanism index (m) of $LaAlO_3$ nanopowders

Heating rate (K/min)	nE_c (g mol)	n	m
10	980.68	3.42	2.60
20	966.34	3.37	2.59
30	1003.62	3.5	2.84
40	860.25	3	2.50
Average	952.01	3.32	2.63

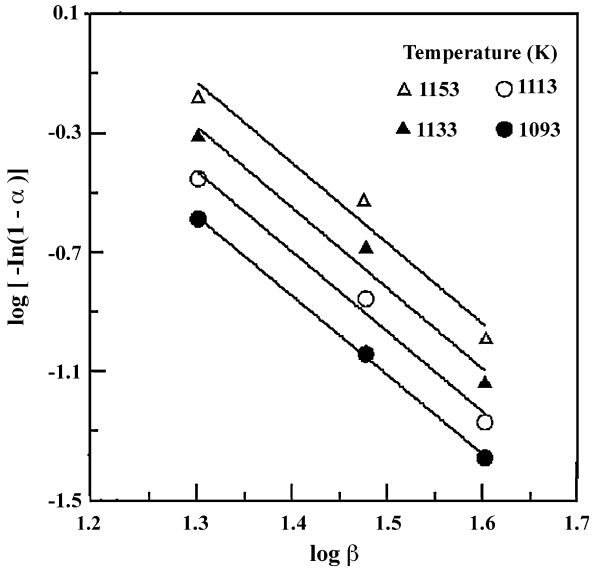

Fig. 7. Relation between $\log[-\ln(1-\alpha)$ and $\ln\beta$ at various temperatures for $LaAlO_3$ powders.

values can also be approximated to 3. These results also indicate that the bulk nucleation dominates in the crystallization and the crystal growth is controlled by diffusion at a fixed number of nuclei in $LaAlO_3$. JMA criterion depicts that $n = 3$ describes three-dimensional growth from a constant number of nuclei and shows a spherical morphology as observed in SEM and TEM images (Figs. 8 and 9).

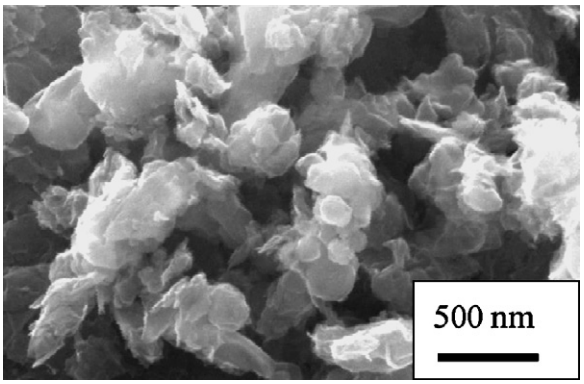

Fig. 8. SEM micrograph of $LaAlO_3$ gel powders calcined at 1083 K for 10 min.

3.3. Microstructure of the rhombohedral $LaAlO_3$ nanopowders

Since the $LaAlO_3$ gel powders are prepared through the wet-chemical route, the agglomeration takes place during processing. Fig. 8 illustrates the typical scanning electron micrograph (SEM) of the $LaAlO_3$ gel powders calcined at 1083 K for 10 min. It indicates the agglomerated nanocrystalline $LaAlO_3$ powders have a spherical morphology with an average diameter of 70 nm. The largest cluster is several micrometers in diameter.

The TEM microstructure and ED pattern of the $LaAlO_3$ gel powders calcined at 1083 K for 10 min are shown in Fig. 9. Fig. 9(a) shows the bright field (BF) TEM micrograph of the $LaAlO_3$ nanocrystallites, indicating that the nanocrystalline $LaAlO_3$ powders have a spherical morphology with an average diameter ranging from 20 to 30 nm. Moreover, the rhombohedral $LaAlO_3$, marked "X" in Fig. 9(a), has been identified by SAED in Fig. 9(b), illustrating that the $LaAlO_3$ has a zone axis of $[1\,\bar{1}\,\bar{1}]$.

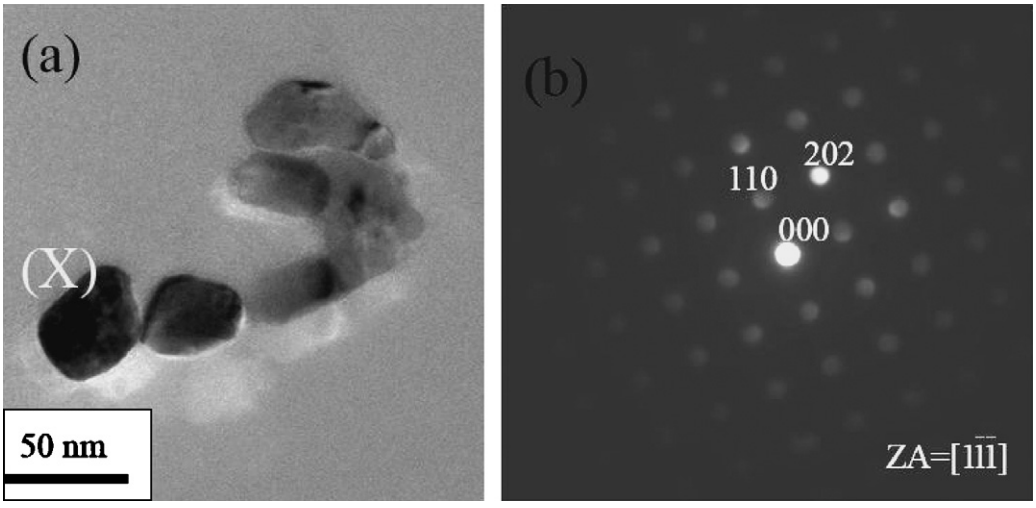

Fig. 9. TEM image and SAED pattern of $LaAlO_3$ gel powders calcined at 1083 K for 10 min: (a) BF image, and (b) SAED patterns of $LaAlO_3$ with ZA = $[1\,\bar{1}\,\bar{1}]$.

4. Conclusion

The crystallization kinetics and growth mechanism for the crystallization of $LaAlO_3$ gel powders have been investigated using DTA, SEM, TEM and SAED. The results are summarized as follows:

(1) The non-isothermal activation energy for the crystallization of $LaAlO_3$ gel synthesized by chemical co-precipitation method is found as 286.75 kJ/mol.
(2) The growth morphology parameter (n) and crystallization mechanism index (m) are both approximated as 3 indicating three-dimensional growth from a constant number of nuclei, and a spherical morphology.
(3) Both TEM examination and SAED analysis also indicate that the cubic $LaAlO_3$ with a spherical morphology ranges from 20 to 30 nm.

References

[1] T. Ishihara, K. Shimose, T. Kudo, H. Nishiguchi, T. Akbay, Y. Takita, Preparation of yittria-stabilized zirconia thin films on strontium-doped $LaMnO_3$ cathode substrate via electrophoretic deposition for solid oxide fuel cells, J. Am. Ceram. Soc. 83 (2000) 1921–1927.
[2] G.Y. Sung, K.Y. Kang, S.C. Park, Synthesis and preparation of lanthanum aluminate target for radio-frequency magnetron sputtering, J. Am. Ceram. Soc. 74 (1991) 437–439.
[3] M. Mizuno, T. Yamada, T. Noguchi, Phase diagram of the system Al_2O_3–La_2O_3 at high temperatures, Yogyo Kyokaish 82 (1974) 630–636.
[4] E. Taspinar, A.C. Tas, Low-temperature chemical synthesis of lanthanum monoaluminate, J. Am. Ceram. Soc. 80 (1997) 133–141.
[5] W. Li, M.W. Zhuo, J.L. Shi, Synthesizing nano $LaAlO_3$ powders via co-precipitation method, Mater. Lett. 58 (2004) 365–368.
[6] K. Vidyasagar, J. Gopalakrishnan, C.N.R. Rao, Synthesis of complex metal oxide using hydroxide cyanide, and nitrate solid-solution precursor, Bull. J. Solid State Chem. 58 (1989) 29–37.
[7] A. Douy, P. Odier, Polycrylamide gel: a novel route to ceramic and glassy oxide powders, Mater. Res. Bull. 24 (1989) 1119–1126.
[8] M. Kakihana, T. Okubo, Low temperature powders synthesis of $LaAlO_3$ through in situ polymerization route utilizing citric acid and ethylene glycol, J. Alloys Compd. 266 (1998) 129–133.
[9] C.L. Kuo, C.L. Wang, T.Y. Chen, G.J. Chen, I.M. Hung, C.J. Shih, K.Z. Fung, Low temperature synthesis of nanocrystalline lanthanum monoaluminate powders by chemical coprecipitation, J. Alloys Compd. 440 (2007) 367–374.
[10] M. Chroma, J. Pinkas, I. Pakutinskiene, A. Beganskiene, A. Kareiva, Processing and characterization of sol–gel fabricated mixed metal aluminates, Ceram. Int. 31 (2005) 1123–1130.
[11] S.K. Behera, P.K. Sahu, S.K. Pratihar, S. Bhattacharyya, Low temperature synthesis of spherical lanthanum aluminate nanoparticles, Mater. Lett. 58 (2004) 3710–3715.
[12] A. Marotta, A. Buri, F. Branda, S. Saiello, in: J.H. Simmons, D.R. Uhlmann, G.H. Beall (Eds.), Nucleation and Crystallization in Glasses, The American Ceramic Society, Westerville, OH, 1981, p. 146.
[13] A. Marotta, A. Buri, Kinetics of devitrification and differential thermal analysis, Therm. Acta 25 (1978) 155–160.
[14] H.J. Borchardt, F. Daniels, The application of differential thermal analysis to the study of reaction kinetics, J. Am. Chem. Soc. 79 (1957) 41–46.
[15] K. Matusita, T. Watanabe, K. Kamiya, S. Sakka, Viscosities of single and mixed alkali borate glasses, Phys. Chem. Glasses 20 (1980) 78–84.
[16] K. Matusita, M. Tashiro, Rate of homogeneous nucleation in alkali disilicate glasses, J. Non-Cryst. Solids 11 (1973) 471–484.
[17] K. Matusita, S. Sakka, Y. Matsui, Determination of the activation energy for crystal growth by differential thermal analysis, J. Mater. Sci. 10 (1975) 961–966.